Development of Hydraulic Hazard Mapping within a GIS Environment: Interoperability Between HEC-RAS and QGIS

Biagio Saya[1,*]

[1]Independent Researcher / Licensed Professional Engineer,
Order of Engineers of Messina, Reg. No. 4604, Messina, Italy
[*]Corresponding Author Email: biagiosaya@gmail.com

Presented at the 19th National GIT Conference
Geosciences and Information Technologies Section, Geological Society of Italy
Milazzo (ME), Italy — June 16–18, 2025

Abstract

Alluvial events represent some of the most destructive natural hazards threatening human civilization. Over recent decades, the frequency of extreme rainfall has exposed the Italian territory to periodic and highly damaging inundations, resulting in a dramatic escalation of financial losses and mortality rates. In regions such as Sicily, several industrial and artisanal clusters are strategically yet precariously situated adjacent to natural river embankments, continuously exposing them to high flood risks. Consequently, determining advance flood velocity thresholds across varying return periods, along with precise water depth metrics, is critical for localized risk mitigation. This paper outlines an integrated methodological framework that pairs advanced hydraulic numerical modelling with Geographical Information Systems (GIS) to execute robust hydraulic susceptibility analyses. Integrating hydraulic simulation data into QGIS yields high-resolution flood zoning maps that link physical hydraulic variables to regional vulnerability indices. Crucial spatial input layers, including topography (high-resolution LiDAR DTM/DSM), biology (riparian flood plain vegetation roughness), and bed-load granulometry, serve as fundamental parameters determining channel frictional coefficients. To demonstrate the interoperability of HEC-RAS and QGIS, a real-world application is presented along the Rosmarino River axis. The results illustrate how localized hydraulic outputs can be smoothly post-processed via Raster Calculators into statutory hazard zoning bands (P_1 to P_4), establishing a scientific tool for public territorial planning and Civil Protection execution.

Keywords: Hydraulic Hazard Mapping, HEC-RAS, QGIS Interoperability, LiDAR DTM, Shallow Water Equations, Flood Susceptibility, Rosmarino River.

1. Introduction

Alluvial phenomena represent a persistent and globally escalating threat to infrastructure, economic stability, and human life. Within the Mediterranean basin, and specifically across the Italian peninsula, climatic shifts have accelerated the frequency of short-duration, high-intensity precipitation events. These events yield flash floods that rapidly overwhelm natural drainage networks. The Sicilian territory, characterized by steep mountainous catchments that transition abruptly into densely populated coastal plains, is highly susceptible to these hydro-geological hazards. Industrial, commercial, and artisan hubs are frequently established in historical alluvial plains or in immediate proximity to river channels, elevating regional structural vulnerability.

To safely manage these areas, public administrators and engineers require predictive tools that go beyond historical record inventories. Modern flood hazard mitigation depends heavily on numerical hydraulic models that simulate inundation dynamics across predefined return periods ($T = 50$, 100, and 300 years). Evaluating cross-sectional parameters like water surface elevations (H), flow velocities (V), and wave propagation speeds allows authorities to implement proactive spatial planning and structurally secure urban zones.

2. Methodological Framework

The complete operational workflow for evaluating flood susceptibility and executing hazard zoning consists of five distinct technical phases:

1. **Physical Environment Characterization:** Gathering of morphological, geological, and biological spatial data representing the river basin.
2. **Historical and Inventory Analysis:** Documenting past flooding events, identifying morphological changes, and mapping historical high-water marks.
3. **Hydrological Analysis:** Simulating rainfall-runoff relationships, calculating peak hydrographs (Q_T), and extracting flood volume properties using extreme value statistical distributions.
4. **Hydraulic Modelling:** Executing numerical routing algorithms to transform flow rates into spatial depth and velocity layers.
5. **Hazard Perimetration:** Exporting numerical outputs into GIS to isolate and delineate regulatory hazard boundaries according to legislative standards.

2.1. Flood Hydrograph Dynamics

A flood wave represents a rapid, significant expansion of a watercourse's discharge rate driven by concentrated rainfall or rapid snowmelt, followed by a gradual recession back to baseflow conditions. Analytically, a hydrograph depicts this volumetric flow rate change over time, capturing the rising limb, peak flow, and receding limb (as conceptualized in Figure 1).

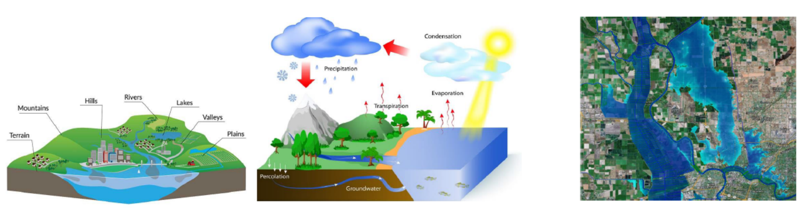

Figure 1: Conceptual overview of flood hydrograph components, demonstrating the asymmetric rise and structural attenuation phases of localized peak flows.

To model the true impact on low-lying infrastructure, unsteady flow analysis tracks the downstream propagation of the hydrograph peak. When an unmanaged flood wave encounters a storage reservoir or an expansive floodplain, a natural or artificial "decapitation" of the peak discharge occurs (Q_{30} attenuation), storing a temporary volume within the channel boundaries and lengthening the hydrograph's recession tail.

2.2. National and Regional Legislative Zoning Criteria

The spatial zoning of flood susceptibility is dictated by institutional regulatory frameworks. According to the operational guidelines of the Hydrogeological Setting Plan (*Piano Stralcio di Bacino per l'Assetto Idrogeologico* — PAI) of the Sicilian Region, the territory is classified into predefined risk zones based on institutional probability distributions. As summarized in Figure 2, this operational scheme structures risk indices across 5 core classes: very high hazard (P_4), high hazard (P_3), medium hazard (P_2), moderate hazard (P_1), and generic areas of attention (AA).

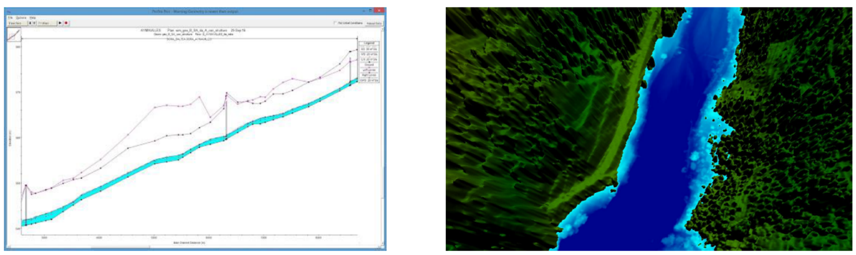

Figure 2: Institutional PAI hazard categorization framework, detailing the division into five key risk levels from P_1 through P_4 and attention areas (AA).

The conversion of raw hydrodynamic parameters into these discrete planning categories requires a dual analytical approach. While standard assessments rely entirely on the return period (T), comprehensive civil protection protocols enforce a joint evaluation matrix that weights local water depth metrics (H) and maximum flow velocity thresholds against the specific event probability.

3. Governing Mathematical Formulations

Predicting spatial flood boundaries requires solving mass and momentum conservation equations. Depending on the complexity of the valley's morphology, two numerical approaches are implemented within the computational routine, shifting from traditional 1D profiles to advanced 2D layouts (Figure 3).

3.1. One-Dimensional Saint-Venant Equations

For steady or confined river reaches where flow vectors align primarily parallel to the channel centerline, the classic 1D Saint-Venant system is applied:

$$\frac{\partial A}{\partial t} + \frac{\partial Q}{\partial x} = q \tag{1}$$

$$\frac{\partial Q}{\partial t} + \frac{\partial}{\partial x}\left(\frac{Q^2}{A}\right) + gA\left(\frac{\partial h}{\partial x} + S_f\right) = 0 \tag{2}$$

where A represents the wetted cross-sectional area, Q is the volumetric discharge, q represents lateral inflow, h is water depth, and S_f is the energy slope calculated via Manning's friction formulation.

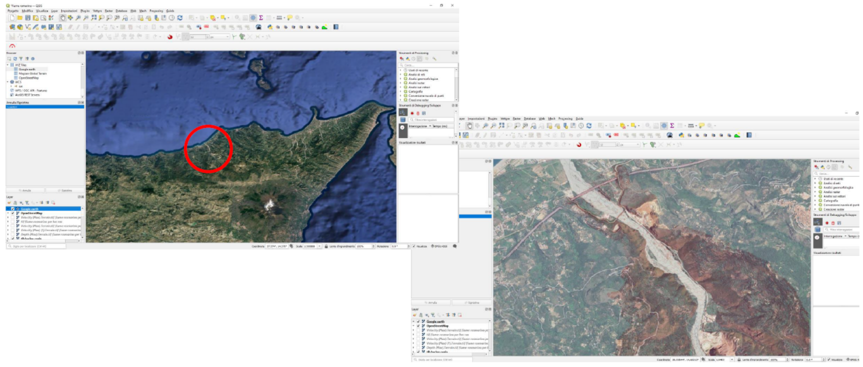

Figure 3: Structural transition in computational fluid mechanics: comparison between classic cross-sectional 1D profiles and fully distributed 2D spatial grid analyses.

3.2. Two-Dimensional Shallow Water Equations (SWE)

In broad, unconfined floodplains, coastal marshes, or complex urban junctions where lateral flow velocity components cannot be ignored, the two-dimensional Shallow Water Equations (SWE), derived from depth-averaging the Navier-Stokes equations, must be resolved (schematized in Figure 4):

$$\frac{\partial(\rho\eta)}{\partial t} + \frac{\partial(\rho\eta u)}{\partial x} + \frac{\partial(\rho\eta v)}{\partial y} = 0 \tag{3}$$

$$\frac{\partial(\rho\eta u)}{\partial t} + \frac{\partial}{\partial x}\left(\rho\eta u^2 + \frac{1}{2}\rho g\eta^2\right) + \frac{\partial(\rho\eta uv)}{\partial y} = -\rho g\eta S_{fx} \tag{4}$$

$$\frac{\partial(\rho\eta v)}{\partial t} + \frac{\partial(\rho\eta uv)}{\partial x} + \frac{\partial}{\partial y}\left(\rho\eta v^2 + \frac{1}{2}\rho g\eta^2\right) = -\rho g\eta S_{fy} \tag{5}$$

where η is the total water column height $(h+z)$, u and v represent depth-averaged velocities in the x and y coordinate directions respectively, ρ is the fluid density, g is gravity, and S_{fx}, S_{fy} are the components of the friction slope along the respective spatial axes.

Figure 4: Mathematical system schematic isolating 2D Shallow Water Equations (SWE) derived from depth-averaging the Navier-Stokes momentum balances.

4. Case Study: Rosmarino River Modelling

The proposed interoperability pipeline was verified along a highly vulnerable reach of the Rosmarino River, located in northern Sicily. The complete computational workflow was managed via direct data exchanges between the RAS Mapper sub-interface of HEC-RAS 6.x and QGIS.

4.1. Topographical Infrastructure Processing via LiDAR DTM

High-resolution terrain inputs were acquired via the National Environmental Data Portal of the Italian Ministry of Environment and Energy Security (MASE), leveraging a public database funded by the European Union under the NextGenerationEU framework (Figure 5). High-density airborne LiDAR data was downloaded as a 1×1 m gridded Digital Terrain Model (DTM).

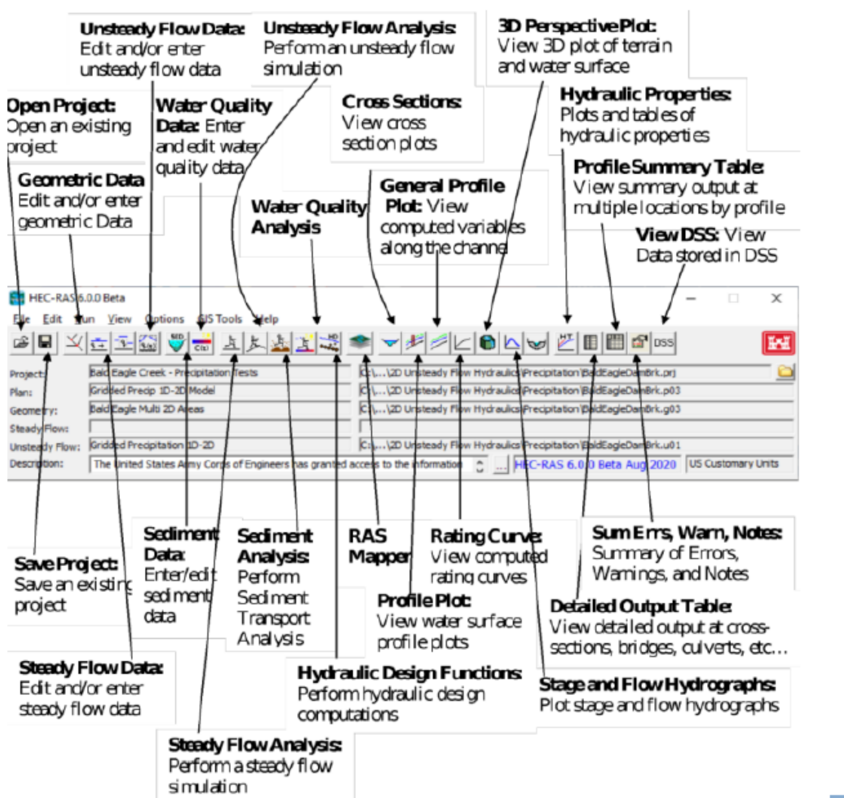

Figure 5: Acquisition phase of high-resolution digital topography within the MASE environmental server interface.

These LiDAR tiles were imported directly into QGIS to confirm spatial projections and coordinate system consistency, verifying the local projection framework against the EPSG:32633 (WGS 84 / UTM Zone 33N) geodetic datum as shown in Figure 6. The unified raster terrain was then linked inside RAS Mapper to create a continuous computational surface.

4.2. Computational Mesh and Boundary Sub-layer Definition

The mathematical routing configuration was initiated by defining the hydraulic simulation domain in the RAS Mapper editor environment (Figure 7). A comprehensive 2D computational flow area boundary was delineated around the river channel and its surrounding floodplains.

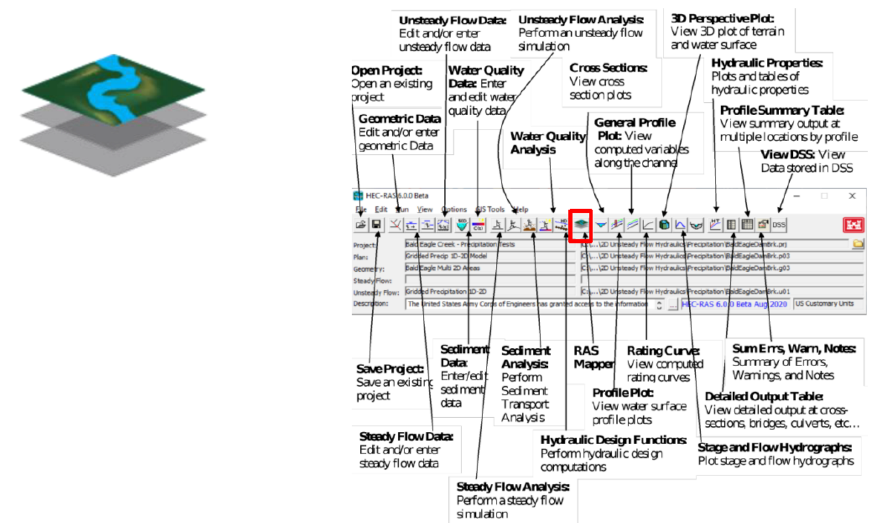

Figure 6: Processing and spatial alignment of the gridded LiDAR DTM layers within the QGIS workspace environment.

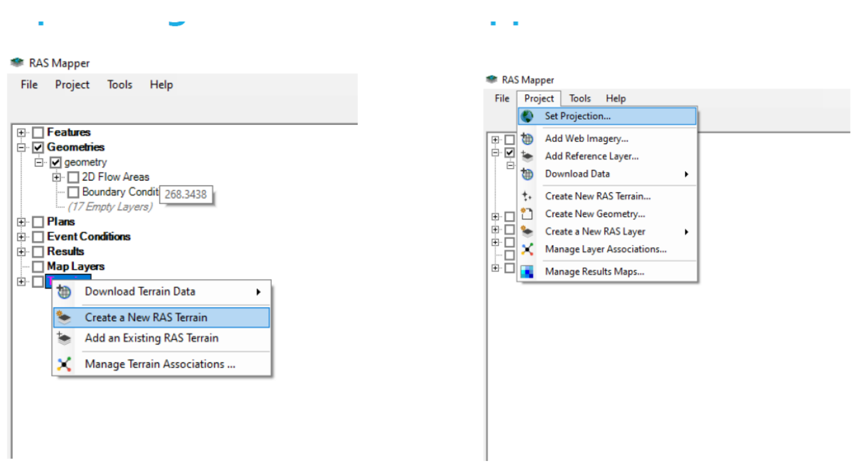

Figure 7: Definition of computational flow domain boundaries and structural elevation models in the RAS Mapper layer manager.

A highly optimized, variable-density integration grid was compiled over the active channel (Figure 8), yielding a continuous computational network where cell dimensions are carefully constrained (minimum area = 19.93 m^2, maximum area = 52.51 m^2). Frictional boundary parameters were assigned using spatially varied Manning's coefficient matrices (n) based on digitized riparian vegetation and gravel bar distributions.

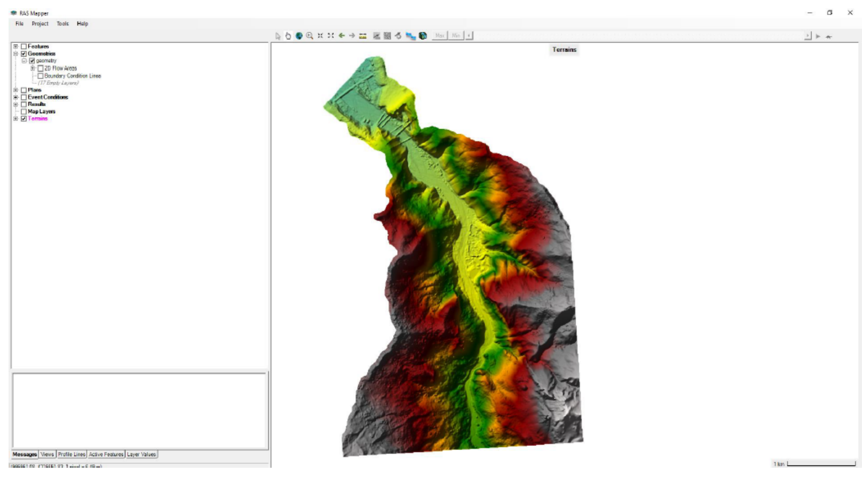

Figure 8: Generation of the finite-volume 2D computational mesh, displaying the integration of geometric boundaries and breaklines over the river bed.

5. Hazard Mapping Results and Discussion

Following unsteady hydraulic execution, maximum water depths ($H_{\max}$) and overflow velocity distributions ($V_{\max}$) were exported from RAS Mapper as georeferenced high-resolution GeoTIFF surfaces. Figure 9 details the localized water surface heights extracted at peak flow, displaying severe lateral expansion over the left embankment.

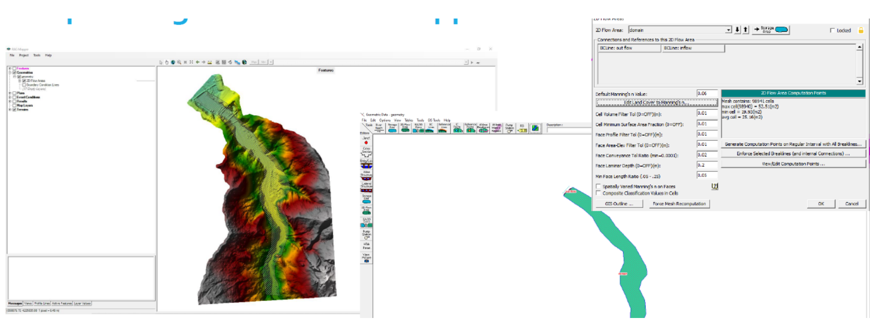

Figure 9: Processed spatial distribution of maximum flood wave depths ($H_{\max}$) computed along the active Rosmarino channel boundaries.

5.1. Regulatory Hazard Matrices

According to the operational guidelines of the Hydrogeological Setting Plan (*Piano Stralcio di Bacino per l'Assetto Idrogeologico* — PAI) of the Sicilian Region, hydraulic hazard classes must be categorized from P_1 (moderate) to P_4 (very high). While simplified approaches depend solely on the return period (T), the comprehensive framework requires evaluating the combined impact of water depth and return period, as configured in Table 1.

Table 1: Regulatory Hydraulic Hazard Matrix (PAI Sicily Framework)

Hydraulic Depth (H)	**Return Period (T)**		
	50 Years	**100 Years**	**300 Years**
$H < 0.3$ m	P_1	P_1	P_1
$0.3 < H < 1.0$ m	P_2	P_2	P_2
$1.0 < H < 2.0$ m	P_4	P_3	P_2
$H > 2.0$ m	P_4	P_4	P_3

5.2. GIS Post-Processing and Raster Calculator Expressions

To classify the raw model outputs into these institutional hazard categories within QGIS, the Raster Calculator was deployed to execute conditional boolean matrices. The continuous map-algebra workflow operates by cross-evaluating depth limits against regional thresholds.

As shown in Figure 10, the spatial extraction maps distinct polygons for each target risk index. The logical stacking of depth and velocity rasters automatically isolates the P_2 (medium) and P_3 (high) hazard zones, mapping them directly onto local industrial and artisan parcels to provide a clear overview of building vulnerability.

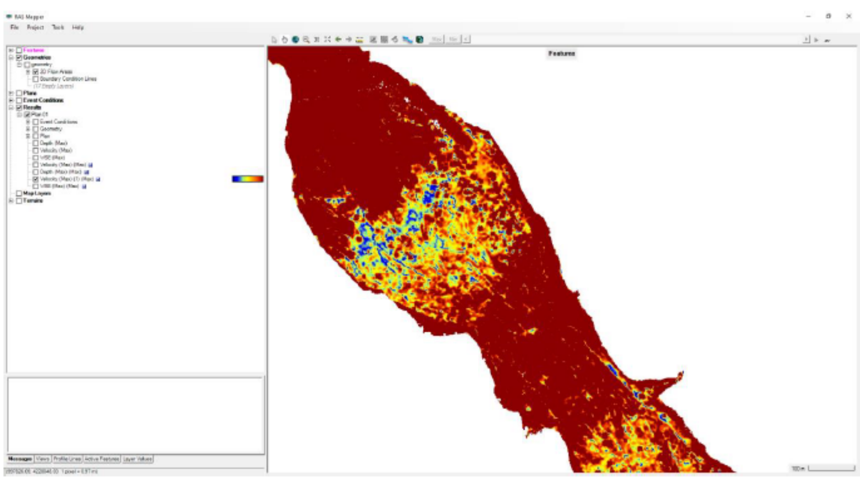

Figure 10: Delineation of institutional hazard bands (P_2 and P_3) generated through conditional map-algebra scripting within the QGIS environment.

6. Conclusion and EarthArXiv Publishing Notes

This research demonstrates the high interoperability between HEC-RAS and QGIS for regional flood risk assessment. Leveraging high-density LiDAR data within an integrated 2D shallow water solver ensures highly detailed representation of flood wave propagation over complex surfaces. This approach provides public planning departments with an empirical tool to update civil protection guidelines and restrict unsafe structural expansion in active floodplains.

EarthArXiv Preprint Policy & Citation Compliance

In accordance with EarthArXiv standards for open-access geoscientific presentation series, this manuscript serves as a reproducible draft of the work presented at the 19th National GIT Conference (Milazzo, 2025).